J Ther Eng, Vol. 10, No. 6, pp. 1440−1452, November, 2024

Journal of Thermal Engineering
Web page info: https://jten.yildiz.edu.tr
DOI: 10.14744/thermal.0000885

Research Article

Experimental estimation of radiation heat losses from a fully open cylindrical cascaded cavity receiver by radiosity network method

Kushal S. WASANKAR[1,*], Nitin P. GULHANE[1]

[1]*Department of Mechanical Engineering, VJTI, Mumbai, 400019, India*

ARTICLE INFO

Article history
Received: 01 August 2023
Revised: 09 December 2023
Accepted: 06 January 2024

Keywords:
Cavity Inclination; Cavity Receiver; Heat Losses; Parabolic Dish; Radiosity Network; Solar Concentrators

ABSTRACT

The performance of solar thermal power systems using cavity receivers and parabolic dishes highly depends on the effective absorption of concentrated solar radiation by cavity receivers. Correct measurement of convection losses is challenging due to non-isothermal surface temperatures and unpredictable flow conditions inside the cavity. Correct prediction of radiation losses can help to predict convection losses. Effect of increasing the area ratio of normal cavity using cylinder in cylinder arrangement to increase the surface area for heat transfer, is studied experimentally. The specially designed heaters for model cavity size using nichrome wires sheathed between ceramic sheets were used to apply the thermal load, and the heat transfer rate was observed. Experimental temperatures were used for calculating the radiation heat losses using radiosity network method. Modified cavity surface is divided in parts and radiosity values for each part is calculated by solving simultaneous equation obtained by network method, using Gauss-Seidel method. Finally, the radiation heat loss from each surface is added to get total radiation heat loss. More heat transfer area for cylinder in cylinder arrangement and with the same heat input modified cavity shows higher surface temperatures. Network representation provides a better understanding of radiative interaction between different parts of the cavity. Radiosity network method predicts more accurate results than mean radiation heat loss calculations by calculating actual radiosity values for different parts of cavity. The difference in prediction is high at lower temperatures, emissivity and reduces with increasing temperature and emissivity. Effect of inner cylinder surface temperature was studied with three different cases and found that the radiation heat losses are less affected by inner cylinder surface temperatures. Effect of aspect ratio on radiation heat losses is presented in this work. Experimental results show that proposed cavity receiver design provide double surface area for heat transfer with increased surface temperatures for same heat input and total heat loss.

Cite this article as: Wasankar KS, Gulhane NP. Experimental estimation of radiation heat losses from a fully open cylindrical cascaded cavity receiver by radiosity network method. J Ther Eng 2024;10(6):1440−1452.

***Corresponding author.**
*E-mail address: wasankark@gmail.com

This paper was recommended for publication in revised form by Editor-in-Chief Ahmet Selim Dalkılıç

Published by Yıldız Technical University Press, İstanbul, Turkey
Copyright 2021, Yıldız Technical University. This is an open access article under the CC BY-NC license (http://creativecommons.org/licenses/by-nc/4.0/).

INTRODUCTION

In near future, the demand for energy will increase significantly with increase in industrialization and upgraded living standard of the society. Most of the energy demand in today's scenario is fulfilled by conventional fuels like coal, diesel, LPG and CNG etc. But with the increasing consumption of fossil fuel, their availability in near future is questionable. Their prices are increasing and also, they have very high impact on environment due to air, land and water pollution associated with their use. Only unconventional energy sources like solar and wind energy, can provide us the solution for required energy demand along with lesser environmental effects.

Wind energy availability will depend on atmospheric conditions and location on the earth. Whereas solar energy is available on most of the part of the earth at least during the day hours and we can store it to use during night hours. Solar energy has various advantages like free of cost, abundant availability, safe to use and most important is nonpolluting energy. After all sun is the source of energy for all living beings on the earth.

In last few decades, we are using solar PV panels for producing electrical energy. But the problem of electrical energy storage with associated cost, battery life and low efficiency has restricted its use. Flat plate solar collector's use is also restricted to low temperature applications like domestic water heaters and industrial heating applications only. Concentrated solar thermal systems may provide the solution for medium and high temperature applications like process heat and electricity generation.

Concentrating solar dish technology is one of the practical configurations for utilizing solar energy for industrial heat. The receivers used are of cylindrical or cavity type, which converts solar energy into thermal energy. These receivers are positioned at the dish's focus, allowing for the collection of concentrated solar irradiation. Compared to cylindrical receivers, cavity receivers are expected to have reduced convection and radiation heat loss to the environment due to their lower view factor to the surroundings [1]. It is widely acknowledged that of the conduction, radiation, and convection losses from solar cavity receivers, the determination of convection losses is the most complex [2]. Various cavity shapes, like cubical, rectangular, cylindrical, and hemispherical, have been reported in the literature. However, the rectangular cavity is the most popular and widely utilized by many researchers.

Paitoonsurikarn and Lovegrove [3] presented the comparison of numerical results for cylindrical and conical cavity with earlier correlations whereas Paitoonsurikarn Lovegrove [4] presented numerical study for cylindrical and conical cavity under natural convection. Alvarado-Juárez et al. [5] studied the square cavity receiver and reported natural convection and radiative heat transfer as predominant heat transfer phenomenon. Maurya et al. [6] has reported that evaluation of convection and radiative heat losses are essential to improve the thermal performance of solar power system. Wu et al. [7] studied the cylindrical cavity receiver for different boundary conditions and reported natural convection to be more sensitive to tilt angle than radiation and conduction heat transfer. Loni et al. [8] experimentally studied different cavity designs and found that hemispherical and cubical cavities are the most effective designs, while the cylindrical cavity presents lower performance. Eterafi et al. [9] used conical cavity receiver with an ultra-white glass covering the aperture and reported improvement in useful energy absorbed due to glass cover.

Gonzalez et al. [10] considered a square open cavity of length L in 2 dimensions for natural convection and solar radiation; boundary conditions were similar to Juarezb et al. [11]. The fluid was radiatively non-participating, and the cavity walls were considered black bodies. The ambient fluid is air at atmospheric pressure and was assumed Newtonian and an ideal gas. The fluid flow was assumed to be laminar and at a steady state. To calculate the radiative heat flux, the view factor is calculated using Hottel's crossed string method (Modest 1993). Temperature dependant properties of working fluid were considered.

Venkatachalam and Cheralathan [12] conducted experiments on a conical receiver made from a mild steel tube coiled spirally for three different aspect ratios of 0.8, 1, and 1.2. Smaller the size of the receiver, the greater the concentration ratio, and hence the average concentrated flux increases. However, the receiver dimensions cannot be reduced below the size of the focal image as the intercept factor reduces. Yuan et al. [13] conducted the experimental investigation with cylindrical cavity receivers with bottom surface interior convex for different heights of interior convex. They compared the optical efficiency of the receivers. They observed that the optical efficiency values would be higher for the h/H ratio of 0.625, where 'h' is the height of the interior convex and 'H' is the depth of cavity receiver. The thermal efficiency of the receiver with interior convex is increasing with increasing h/H, and a maximum increase of 4.1 % is observed at h/H of 0.875.

Bellos et al. [14] carried out the optical and thermal analysis of different cavity receiver designs and found that the cylindrical, conical design gives the best performance, and cylindrical cavity performance will be slightly less than this. They have also reported the effect of aspect ratio on thermal efficiency and optical efficiency. They found that both the efficiencies will have maximum value at an aspect ratio of slightly more than 1, and with an increasing aspect ratio, thermal efficiency reduces and optical efficiency increases. The reason for the thermal efficiency reduction with the cavity length increase is based on the higher outer surface of the cavity, and higher cavity length increases the absorption of the incoming solar rays into the cavity, and thus, the optical efficiency increases as the cavity length increases. A higher cavity length captures more secondary reflections inside the cavity, which is beneficial for the cavity from the optical point of view. Reddy and Kumar [15]

studied the effect of two-stage concentration using secondary reflectors of various shapes on the thermal performance of spherical cavity receivers. They observed that the cone shape secondary reflector gives lesser convection heat loss, but the trumpet shape gives the best performance with reference to total heat loss.

Reddy and Kumar [16] studied the combined laminar natural convection and surface radiation heat transfer in a hemispherical cavity with all the surfaces covered by tubing. To account for radiation exchange in an internal surface, surface to surface (S2S) model is coupled with the laminar natural convection model. The surfaces are considered gray and diffuse in the surface-to-surface radiation model. The emissivity and absorptivity of a gray surface are independent of the wavelength. The reflectivity is independent of a diffuse surface's outgoing (or incoming) directions. The energy exchange between two surfaces depends on their size, separation distance, and orientation. A view factor accounts for the influences of these parameters. The primary assumption of the surface-to-surface model is that the absorption, emission, and scattering of radiation by the working fluid have yet to be considered [16].

Ibrahim and Salleh [17] analysed the effect of radiation heat transfer inside the oven under natural convection mode using the network representative method. From the surfaces involved, they derived the electrical network based on surfaces to surfaces that absorbs and transmits radiation. An electrical network represents the exchange process between surfaces. The network representation of a single surface and all surfaces together was well explained, and this technique can be easily adapted for our proposed receiver for radiation heat loss analysis.

One of the effective methods for calculating heat exchange between diffuse surfaces of the solar receiver is radiosity analysis which is previously introduced by Holman [18]. Radiosity is the quantity that represents the rate at which radiation energy leaves a unit area of the surface in all directions. Taumoefolau et al. [19] and Maag et al. [20] used radiosity method in calculating the losses from the solar receiver irrespective of size and shape. Neber and Lee [21] used radiosity and Zou et al. [22] used effective absorptance for calculating radiation heat losses form the cavity. Bader et al. [23] applied net radiation method for calculating radiative heat exchange and Monte Carlo ray tracing method for optical efficiency. Hathaway et al. [24] applied Monte Carlo ray tracing to evaluate the impact of the geometry and the spectral characteristics of the surface on the absorption efficiency and the spatial distribution of temperature. Pye et al. [25] used optical ray-tracing for incident solar flux, radiosity analysis for thermal emissions. Gil et al. [26] developed a thermal model using Engineering Equation Solver software by combining radiosity analysis with the finite difference method. Such approaches are based on the assumption of uniform radiosity over the receiver surface. Abbasi-Shavazi et al. [27] have developed a new Nusselt correlation by experimental investigation performed on a non-isothermal scale-model cylindrical cavity receiver. They used a radiosity network method. The view factors of all surface-to-surface configurations were obtained along with radiosity at each node of the cavity receiver.

Furthermore, Wang et al. [28] combine radiosity analysis with photogrammetry and image recognition techniques to evaluate the directional and special radiosity of the solar thermal receiver. Based on it, the radiation losses from the receiver were determined by calculating the reflection losses. Sinha and Gulhane [29] have implemented a quantitative analysis of total radiation heat loss from a cavity receiver using a network method. Such an approach is based on non-uniform radiosity over the entire cavity surface. The Gaussian elimination method is used to solve and estimate the total radiation heat loss from the cavity.

A typical cylindrical cavity receiver design is modified to increase the area ratio in the form of a cylinder-in-cylinder arrangement to determine the effect on various heat losses from the receiver. Wasankar et al. [30] has carried out the numerical investigation for increased area ratio and found promising results with increased cavity surface temperatures. Numerical results were compared with experimental results of Abbasi-Shavazi et al. [27] and they were in close agreement. They found maximum of 18 % reduction in convection heat losses at 0^{o} inclination for modified cavity. The area ratio is doubled in modified cavity by inserting the inner cylinder, and its height is adjusted. The experimental setup was designed and fabricated to measure the surface temperature at various locations under constant heat flux input conditions. The specially designed heaters for model cavity size using nichrome wires sheathed between ceramic sheets were used to apply the thermal load, and the heat transfer rate was observed. These temperature values are then used for calculating the radiation heat loss from the receiver using the radiosity network method. A comparison of radiation heat loss calculation using uniform radiosity and non-uniform radiosity for isothermal surface condition, effect of surface emissivity, aspect ratio on radiation heat losses and experimental results for non-isothermal surface conditions are presented in this paper.

RADIOSITY NETWORK METHOD

For simple problems that involve only a few surfaces, the network method affords a solution that can be easily obtained. When many heat-transfer surfaces are involved, it is to our advantage to formalize the procedure for writing the nodal equations. For the non-uniform radiosity over a heated cavity surface, the inner area of the cavity should be divided into an i_{th} number of surfaces (areas), and radiation heat loss from each surface is calculated by using the radiosity values for that surface. The heat loss thus calculated from each surface is to be added to get the total radiation heat loss from the cavity's inner heated surface.

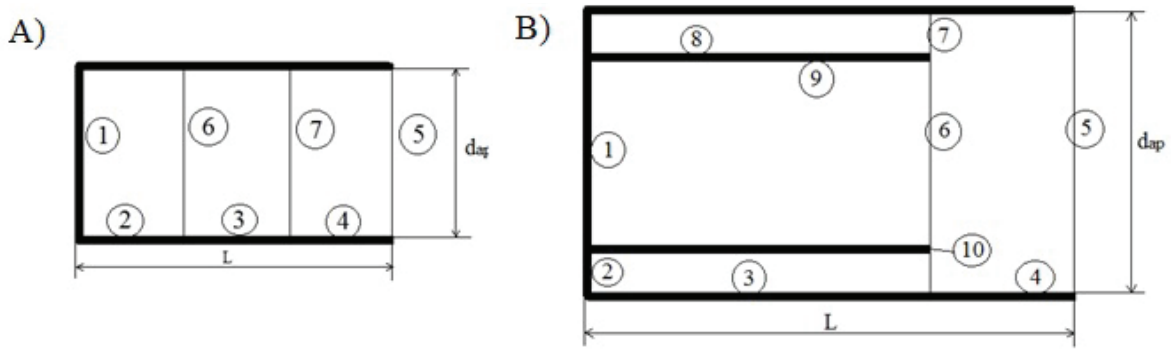

Figure 1. Cavity receiver designs: (A) Normal cavity with 7 surfaces considered for total radiation heat loss calculations (B) Designation of various surfaces for proposed cavity.

The Methodology Used for the Radiosity Network Method

Figure 1 shows the normal cavity and cascaded cavity receiver. The radiosity network method can be implemented through following steps.

1. Divide the cavity surface area by an i_{th} number of surfaces as shown in Figure 1(A) and (B).
2. Evaluate F_{ij} and emissivity ε_i for all surfaces.
3. Evaluate black body emissive power E_{bi} for all surfaces with specified temperature T_i measured from experiments.
4. Formulate nodal equations for the radiosities Ji for each surface using equations (14,15). Please Note that for surfaces in radiant balance $J_i = E_{bi}$.
5. Solve the set of equations for radiosity by direct (Matrix inverse) or iterative methods like the Gaussian elimination method or Gauss-Seidel method.
6. Calculate the heat loss q_i from i_{th} surfaces using equation (19) for gray surfaces and equation (20) for black surfaces with specified temperature T_i.

Calculate Ti for the surfaces in radiant balance using

$$J_i = E_{b_i} = \sigma T_i^4 \quad (1)$$

For Surfaces with specified q_i, find Ti using $E_{b_i} = \sigma T_i^{\,4} = J_i + \frac{1-\varepsilon_i}{\varepsilon_i}\frac{q_i}{A_i}$

7. Add all the radiation heat loss q_i from all the i_{th} surfaces to find the total radiation heat loss from the cavity surface.

Modeling Total Radiation Heat Loss for Cascaded Cavity

The proposed cavity is first divided into ten different surfaces to simplify the procedure of calculating various view factors for each surface with other surfaces. The designation of surface numbers is shown in Figure 1(B). The emissivity value for non-painted and painted cavity surface conditions are 0.6 and 0.87, respectively. For this analysis, the following assumptions are considered:

1. The cavity surfaces are assumed to be gray, opaque, and diffused.
2. Each cavity surface is assumed to be isothermal and with uniform radiosity.
3. The aperture is assumed to be a black surface.

The network representation method shows interactions between different cavity surfaces for calculating total radiation heat loss. The radiative heat balance is represented in a network form. Compared to an electric network, E_{bi} and J_i will be analogous to the potential; q_i and R_i will be analogous to the current and resistances, respectively. A radiation network is constructed by identifying nodes associated with the radiosities of each surface. Then each radiosity node is connected to the other radiosity nodes via the equivalent resistances. Finally, the blackbody emissive powers associated with the temperature of every surface to the J_i nodes are connected through surface resistance. The complete network involving all surfaces of the proposed cavity is shown in Figure 2.

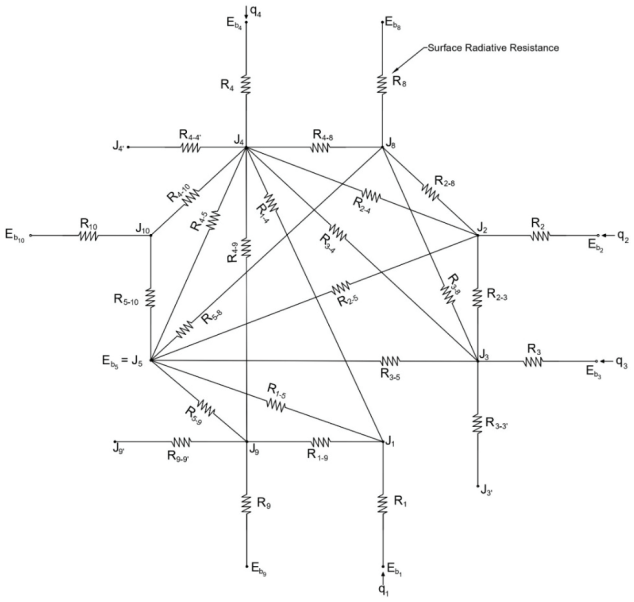

Figure 2. Network representation for all the surfaces inside the proposed cavity.

The following equations give the radiative surface resistance and radiative space resistance.

$$R_i = \frac{1-\varepsilon_i}{A_i \epsilon_i} \quad (2)$$

$$R_{ij} = \frac{1}{A_i F_{ij}} \quad (3)$$

As we have the dimensions and area of all the cavity surfaces, we can find out the view factor using the reciprocity theorem, summation rule, symmetry, and the charts provided by Holman [18]. Dimensions of the cavity used for calculating view factors and material properties used are given in Table 1.

Table 1. Cavity dimensions and material properties

Nomenclature	symbol	value or dimension
diameter of the cavity receiver	D_{cav}	0.083 m
length of cavity	L	0.166 m
length of the inner cylinder in case of cascading	L_3	0.116 m
emissivity of the cavity wall surface	ε_w	0.87
ambient temperature	T_{amb}	300 K

At each J_i node, an energy balance gives the nodal equations for the radiosity as

$$\frac{\varepsilon_i}{1-\varepsilon_i}\left(E_{b_i} - J_i\right) + \sum_J F_{ij}\left(J_j - J_i\right) = 0 \quad (4)$$

Radiant heat transfer at each surface is evaluated in terms of radiosity J_j using the equation,

$$J_i - (1-\varepsilon_i)\sum_J F_{ij} J_j = \varepsilon_i E_{b_i} \quad (5)$$

For using the Gauss-Seidel scheme to solve the simultaneous equations, the equation (4) must be organized in explicit form for J_i as

$$J_i = \frac{1}{1-F_{ii}(1-\varepsilon_i)}\left[(1-\varepsilon_i)\sum_{j\neq i} F_{ij} J_j + \varepsilon_i E_{b_i}\right] \quad (6)$$

For a surface in radiant equilibrium, $q_i/A_i = 0$ and $J_i = E_{bi}$ may be substituted into Equation (6) to give

$$J_i = \frac{1}{1-F_{ii}}\sum_{j\neq i} F_{ij} J_j \quad (7)$$

If the problem formulation is to include a specified heat flux q_i/A_i at one of the i_{th} surfaces, then J_i can be calculated as

$$J_i = \frac{1}{1-F_{ii}}\left(\sum_{j\neq i} F_{ij} J_j + \frac{q_i}{A_i}\right) \quad (8)$$

Once all the equations are written for all nodes, they can be expressed in the matrix form as

$$[A][J] = [C] \quad (9)$$

A solution for the radiosities can be found by obtaining the inverse to [A] such that

$$[J] = [A]^{-1}[C] \quad (10)$$

Alternatively, we may use the Gauss-Seidel method to solve the set of equations to get the radiosity values of all surfaces. Once radiosities are known, the radiation heat transfer rate from each i^{th} surface is given by

$$q_i = \frac{\varepsilon_i A_i}{1-\varepsilon_i}\left[\sigma T_i^4 - J_i\right] \quad (11)$$

For the black surface, the radiation heat transfer can be calculated using the equation

$$\frac{q_i}{A_i} = \epsilon_i\left(\sigma T_i^4 - \sum_j F_{ij} J_j\right) \quad (12)$$

The addition of individual radiation loss then obtains the radiation heat loss through the aperture as

$$q_{rad,total} = \sum q_i \quad (13)$$

For our proposed cavity, total radiation heat loss will be given by

$$q_{rad,total} = q_1 + q_2 + q_3 + q_4 + q_8 + q_9 + q_{10} \quad (14)$$

Fabricated Experimental Setup and Experimental Procedure

The proposed cavity size and design were inspired by the cavity used by Abbasi-Shavazi et al. [2]. The same normal cavity size was used for the sake of comparison of experimental results with available results. The electrical heating method will supply uniform heat flux from the outer side of the cavity. Band-type electric resistance heaters were used for side surface heating, whereas the bottom surface was heated with an annular resistance heater. Heaters were made up of nichrome wire sandwiched between ceramic plates from both sides, and the outer side was covered with the help of stainless-steel plates. The power supply to both heaters was controlled manually using two dimmers. 14 K-type thermocouples (measurement uncertainty ± 2.4 K) were used to measure the cavity's inner surface temperature. The inside bottom surface temperature was measured using IR750 infrared thermometer. The cavity was manufactured using stainless steel SS316 grade material. The cavity was held inside the stainless steel SS304 grade enclosure of 300 mm diameter. The cavity inside the surface was coated with Pyromark 2500 solar-grade paint with an emissivity of 0.87. The Space between the heaters and enclosure is filled with ceramic wool to reduce conduction heat losses. An arrangement was provided to tilt the cavity along with the enclosure at a required angle between 00 and 900 in step 150 to

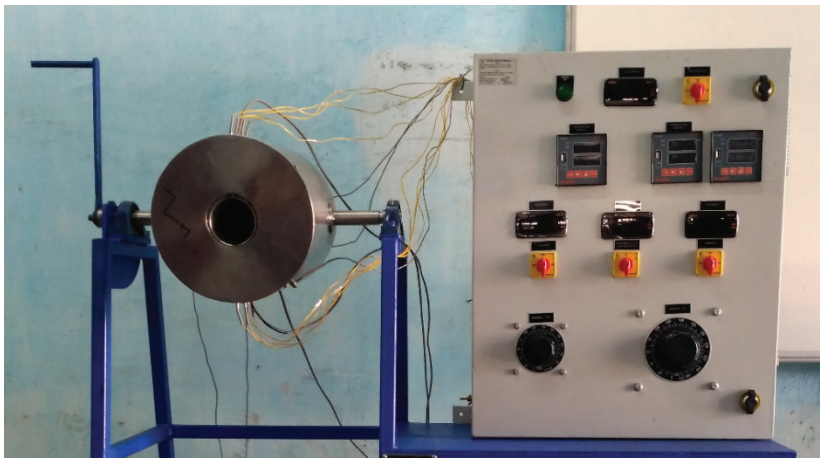

Figure 3. Fabricated setup for experimentation.

study the effect of cavity inclination. The final assembly of the experimental setup is shown in Figure 3. Temperature display has accuracy of ± 0.1 K. Ammeter and voltmeter used were having class 0.5 accuracy.

Using the dimmers, uniform heat flux is applied outside the cavity. The temperature readings were recorded at a steady state when the temperature change recorded by the thermocouple was less than 1 K in one hour. At a steady state, the power delivered by the heaters will be lost by conduction, convection, and radiation. Conduction losses were measured using the material properties and equation proposed by Wu et al. [7]. The radiation heat loss will be calculated using the radiosity network method discussed earlier. The difference between total power supplied and summation of conduction and radiation loss will give us convection heat loss, which is otherwise difficult to measure.

RESULTS AND DISCUSSION

Radiation heat loss calculations using the radiosity network method for non-uniform cavity surface radiosity ($q_{rad\ total}$) and using uniform surface radiosity ($q_{rad\ mean}$) were compared and presented in this section. The effect of cavity wall temperature, emissivity, and aspect ratio on various heat losses from the cavity was presented.

Variation of Radiation Heat Loss with Cavity Wall Temperature

For uniform cavity temperature from 373 K to 1573 K, the estimation of radiation heat loss is carried out for total and mean radiation heat loss. The cavity dimensions and material properties are taken as given in Table 1. Equations 6 and 7 are used to calculate radiosities, equations 11 and 12 are used to calculate heat flux for individual surfaces, equation 14 is used for the calculation of total radiation heat loss, and equation 8 is used to calculate mean radiation heat loss assuming uniform radiosity for all cavity surface. A set of equations for radiosity is solved using the Gaussian elimination method. The mean and total radiation loss percentage difference is calculated using the equation below.

$$\%\ difference\ between\ mean\ and\ total\ radiation\ loss = \frac{(q_{rad\ mean} - q_{rad\ total})}{q_{rad\ mean}} * 100 \quad (15)$$

Figure 4 compares radiation heat loss from the individual surface of the cavity at varying temperatures from 373 K to 1573 K at emissivity of 0.87 and ambient temperature of 300K. Figure 5 compares conduction, mean & total radiation heat losses with % difference for a cascaded cavity at temperature 373-1573 K for the surface emissivity of 0.87 and 300 K ambient temperature. Figure 6 shows the variation of the percentage difference between mean and total radiation heat loss for temperature variation from 373 K to 1573 K and surface emissivity of 0.87.

It is also observed that surface 4 contributes the highest to the radiation heat losses as it is nearer to the aperture and has a high view factor compared to other surfaces. Though

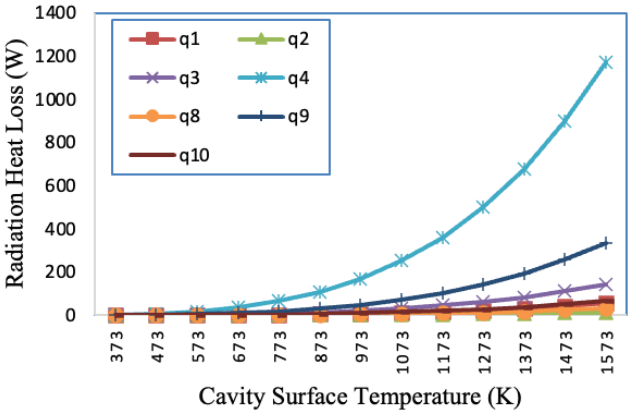

Figure 4. Comparison of total radiation heat loss from the individual surface of the cavity at varying temperatures from 373 K to 1573 K at an emissivity of surface 0.87 and ambient temperature of 300 K.

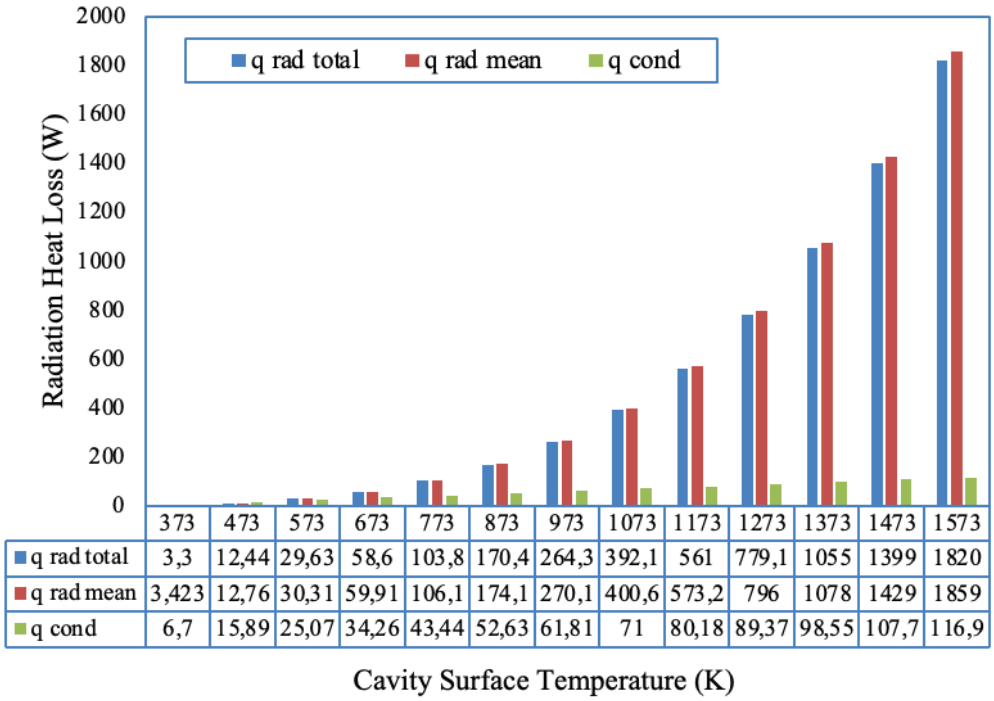

	373	473	573	673	773	873	973	1073	1173	1273	1373	1473	1573
q rad total	3,3	12,44	29,63	58,6	103,8	170,4	264,3	392,1	561	779,1	1055	1399	1820
q rad mean	3,423	12,76	30,31	59,91	106,1	174,1	270,1	400,6	573,2	796	1078	1429	1859
q cond	6,7	15,89	25,07	34,26	43,44	52,63	61,81	71	80,18	89,37	98,55	107,7	116,9

Figure 5. Comparison of conduction and mean & total radiation heat losses for a cascaded cavity at temperature 373-1573 K for the surface emissivity of 0.87 and 300 K ambient temperature.

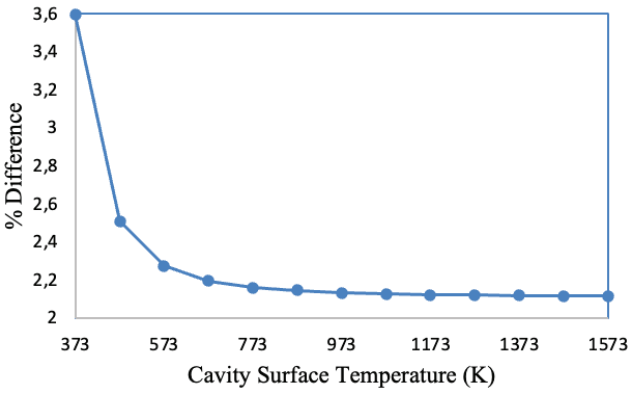

Figure 6. Variation of the percentage difference between mean and total radiation heat loss for temperature variation from 373 K to 1573 K and surface emissivity of 0.87.

the surface area is doubled in the case of the proposed cavity, the radiation heat losses should be theoretically doubled, but due to lower view factors of surfaces 1,2,3,8, and 9, they slightly increase for proposed cavity. So, it is clear that due to the addition of inner cylinder, radiation heat loss from the outer cylinder's inner surface, i.e., surface 3, is significantly reduced due to the lower view factor with the aperture. It was also observed that the radiation heat losses were negligible up to 673 K, then after radiation heat losses increased rapidly.

A comparison of total radiation heat loss for the normal cavity and the cascaded cavity is shown in Table 2 and Figure 7 for three different temperature conditions for an inner and outer cylinder of the cascaded cavity. Case 1: Both are at the same temperature, case 2: constant temperature difference of 25 K between the inner and outer cylinder, and case 3: the increasing temperature difference between the inner and outer cylinder with starting difference of 10 K at 373 K and an increase of 5 K in temperature difference for an increase of 100 K in outer cylinder temperature.

For case 1, the total radiation heat losses are slightly less for the proposed cascaded cavity than the normal cavity at low temperatures. With increasing temperature, the total radiation heat loss will remain nearly the same for both the normal and proposed cavity for all three cases. However, the inner surface area is doubled for the proposed cavity. This means that the insertion of the inner cylinder will not increase the radiation heat loss though the surface area taking part in radiation heat transfer is doubled. Case 2 and case 3 were considered keeping in view that the cavity is heated from the outside, so the outer cylinder will be at a higher temperature than the inner cylinder of the proposed cavity, as we supplied the same power input for both cavities. With all three cases considered here, the total radiation heat losses remain the same and are nearly equal to the losses from the normal cavity. So, the proposed cavity is helping in reducing radiation heat losses though the surface area is doubled. This is because of the lesser view factor of added surface area and reduction in view factor of outer

Table 2. Comparison of total radiation heat loss for normal cavity and cascaded cavity for three different cases

Tempe rature (K)	total radiation heat loss for normal cavity	total radiation heat loss for cascaded cavity (Case 1)	total radiation heat loss for the inner cylinder at 25 K lower temp (case 2)	total radiation heat loss for increasing diff. in inner and outer cylinder temp (case 3)	temperature diff between inner and outer cylinder for case 3
373	3.35	3.30	2.97	3.16	10
473	12.47	12.44	11.74	12.01	15
573	29.63	29.63	28.37	24.96	20
673	58.56	58.60	56.55	56.55	25
773	103.71	103.81	100.68	100.09	30
873	170.22	170.41	165.88	164.18	35
973	263.98	264.30	258.00	254.46	40
1073	391.55	392.06	383.58	377.23	45
1173	560.25	561.00	549.90	539.50	50
1273	778.09	779.14	764.91	748.93	55
1373	1053.77	1055.22	1037.33	1013.90	60
1473	1396.75	1398.68	1376.55	1343.45	65
1573	1817.17	1819.70	1792.70	1747.30	70

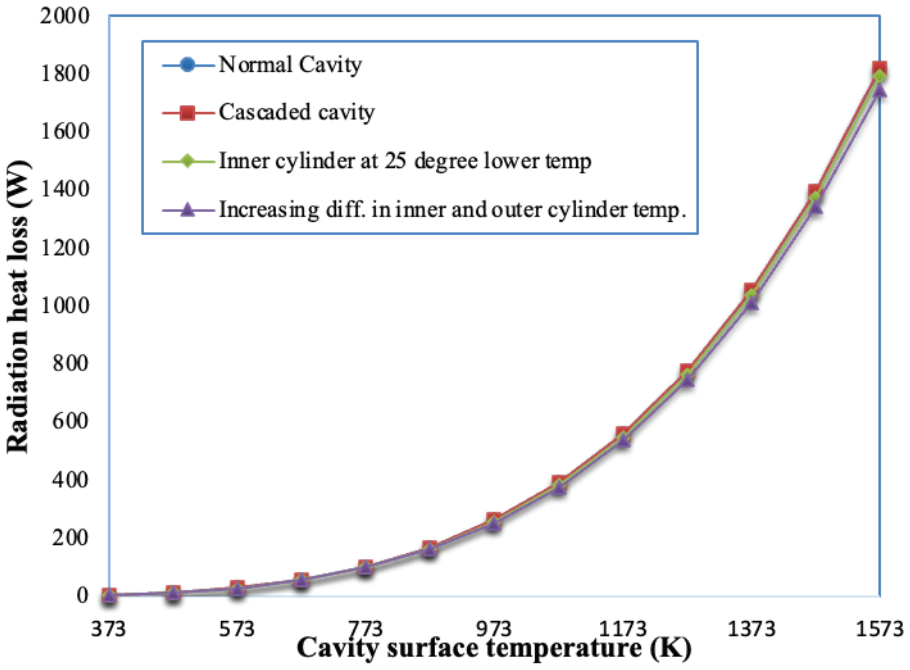

Figure 7. Comparison of total radiation heat loss for normal cavity and cascaded cavity for three different cases.

cylinder area near to bottom of cavity. The annular space between inner and outer cylinder traps the radiations and causes multiple reflection and subsequently absorption of radiation. The inner cylinder surface will have less view factor as it is away from aperture.

Sensitivity Analysis for Proposed Cavity

The effect of emissivity on total and mean radiation heat loss from a cascaded cavity is analysed. Radiation heat loss at a cavity temperature of 873 K is estimated for non-uniform radiosities using equations 6 and 7. The radiosity equations are solved at various emissivity values from 0.2 to 0.9 to estimate the radiation heat loss for different surfaces at a temperature of 873 K. The estimated total and mean radiation heat loss and the percentage difference between mean and total radiation heat loss values are shown Figure 8.

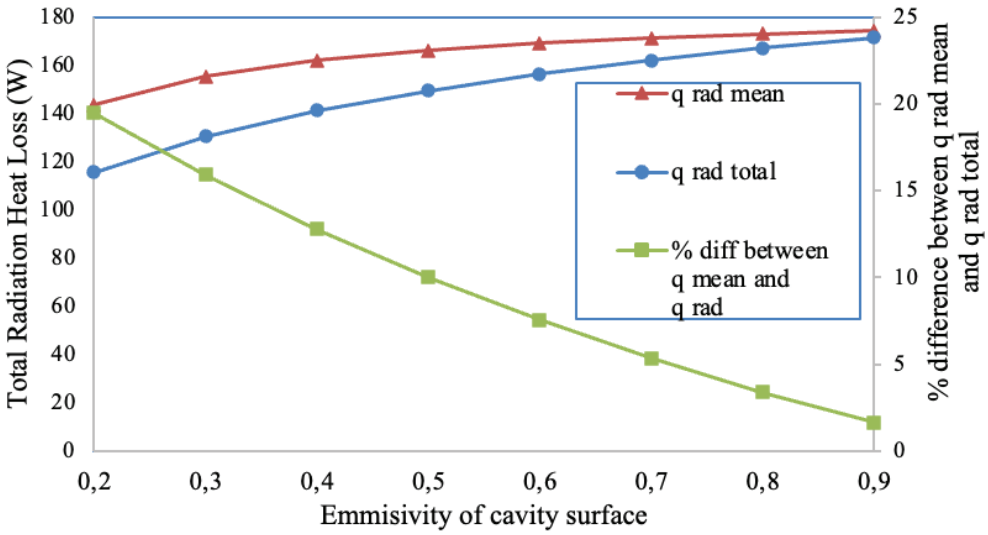

Figure 8. Comparison of total and mean radiation heat loss for the different emissivity of cavity surface at 873 K.

Table 3. Aspect ratio for different cavity lengths

length of cavity (m)	diameter of cavity (m)	aspect ratio
0.083	0.083	1
0.166	0.083	2
0.249	0.083	3

With the increasing emissivity of the cavity surface, the radiation heat losses were increasing for the same uniform surface temperature, which aligns with the general theory of radiation heat transfer. Compared to the radiosity network method, mean radiation heat loss predicts 19.48% higher radiation heat losses for an emissivity of 0.2 and 1.63% higher for an emissivity of 0.9 with a uniform surface temperature of 873K. The radiosity network method calculates radiation losses more accurately than the mean radiation heat loss calculations as it considers non uniform radiosity over cavity surface.

Variation of Radiation Heat Loss with an Aspect Ratio (L/Dcav) of Cavity

To analyze the effect of aspect ratio on radiation heat loss aspect ratio range considered for the study is shown in Table 3. The aspect ratio of the cavity is changed by changing the length of the cavity, and the aperture diameter is kept constant as shown in Table 3. The length of the inner cylinder is chosen such that the area of the cavity surface will get doubled. The temperature of the cavity surface is considered uniform at 873 K and 1273 K, and the emissivity of the cavity surface is taken as 0.87. The radiosity equations are solved at 873 K and 0.87 emissivity of the cavity

Table 4. Different heat losses and the percentage difference between mean and total radiation heat loss for cavity wall temperatures of 873 K and 0.87 emissivity

L (m)	Aw (m^2)	aspect ratio	q rad total	q rad mean	q cond (W)	% diff
0.083	0.05397	1	169.322	172.99	28.12	2.12
0.166	0.0975	2	170.41	174.14	52.63	2.14
0.249	0.1406	3	171.11	174.58	77.14	1.98

Table 5. Different heat losses and the percentage difference between mean and total radiation heat loss for cavity wall temperatures of 1273 K and 0.87 emissivity

L (m)	Aw (m^2)	aspect ratio	q rad total	q rad mean	q cond (W)	% diff
0.083	0.05397	1	774.11	790.77	47.74	2.12
0.166	0.0975	2	779.14	796.01	89.37	2.12
0.249	0.1406	3	782.25	798.02	130.99	1.97

Table 6. Different heat losses and the percentage difference between mean and total radiation heat loss for cavity wall temperatures of 873 K and 0.6 emissivity

L (m)	Aw (m²)	aspect ratio	q rad total	q rad mean	q cond (W)	% diff
0.083	0.05397	1	152.84	164.59	28.12	7.125
0.166	0.0975	2	156.55	169.32	52.63	7.52
0.249	0.1406	3	158.56	171.19	77.14	7.37

Table 7. Different heat losses and the percentage difference between mean and total radiation heat loss for cavity wall temperatures of 1273 K and 0.6 emissivity

L (m)	Aw (m²)	aspect ratio	q rad total	q rad mean	q cond (W)	% difference
0.083	0.05397	1	698.745	752.35	47.74	7.14
0.166	0.0975	2	715.78	773.98	89.37	7.54
0.249	0.1406	3	724.87	782.54	130.99	7.38

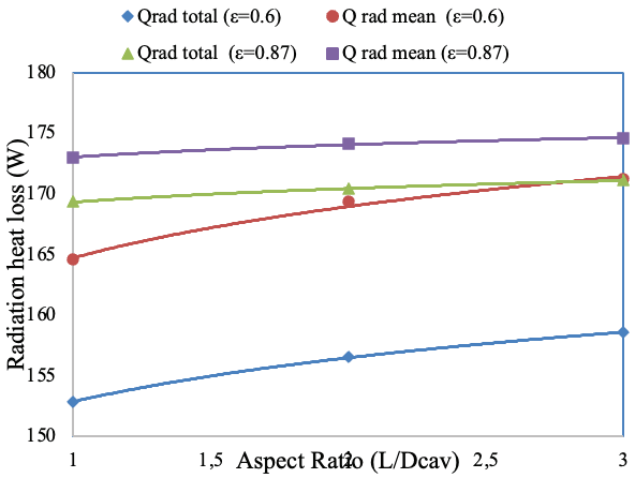

Figure 9. Comparison of total radiation and mean radiation heat loss for cavity surface temperature of 873 K and emissivity of 0.6 and 0.87 for different aspect ratio.

surface to estimate the radiation heat flux values for different cavity surfaces.

Cavity inner surface area, conduction heat loss, mean radiation heat loss, total radiation heat loss, and the percentage difference between mean and total radiation heat loss are given in Tables 4 to 7 for cavity wall temperatures of 873 K and 1273 K, respectively. The emissivity of the cavity wall surface considered for this analysis is 0.6 for the non-painted surfaces and 0.87 for the painted surfaces.

Comparison of total radiation and mean radiation heat loss for cavity surface temperature of 873 K and emissivity of 0.6 and 0.87 for three different aspect ratios are shown in Figure 9. With the increasing aspect ratio, the radiation heat losses increase as the surface area increases. However, the increase is slight as the aperture area is the same for all three cases through which the radiation heat loss occurs. So, increasing the aspect ratio will not significantly increase the radiation heat loss though the surface area is increasing; it is because the increased depth of the cavity accounts for the increased stagnation zone inside the cavity and added area with increased depth of cavity will have lesser view factor.

Radiation Heat Losses for Experimental Surface Temperatures

Experiments were carried out for inclination varying from 0o to 90° in the steps 15° for the cavity coated with Pyromark 2500 (emissivity of 0.87) and heat input of 150 W and 200 W using only side band heaters. An additional case of 150 W heat input using both side and bottom heater were considered for comparison purpose. Experimental temperature values were used to calculate the average surface temperatures for each surface used in the radiosity network method. The radiation heat losses for normal and modified cavity, coated with Pyromark 2500 were calculated using the radiosity network method for different heat input cases presented in Figure 10.

Radiation heat losses will increase for higher heat input conditions as surface temperatures increase. Using only a side heater for a heat input of 150W will show higher radiation heat losses than the same heat input with both bottom and side heaters. As more heat is supplied with the lesser area in case of only side heaters, the surface temperatures are higher. As surface near to aperture contributes maximum to the radiation heat losses, the higher surface temperature of surface 4 in case of only side heater input will result in higher radiation heat losses for this condition. Compared with a normal cavity, a modified cavity shows higher radiation heat losses for all three cases of heat input.

For 150 W input using side heaters only, the maximum radiation loss increase was only 4.5 % for the modified cavity at 15° inclination. The increase is only 2.71 % for 90° inclinations where radiation losses dominate as most of

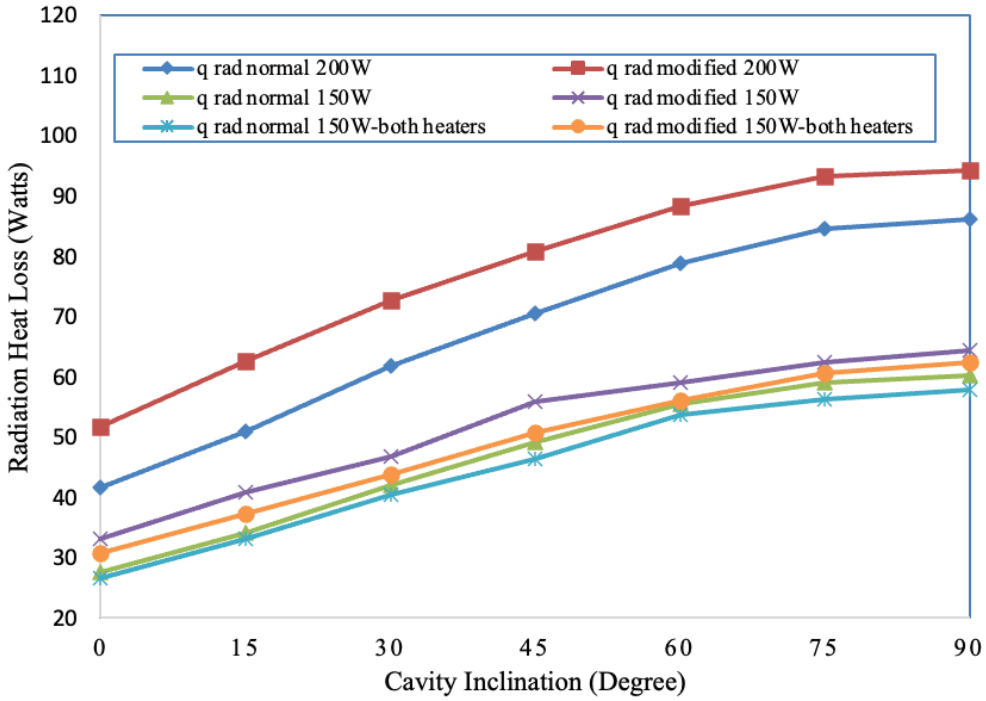

Figure 10. Comparison of radiation heat losses for normal and modified cavities with different heat input conditions for painted cavity (emissivity=0.87).

the cavity region represents a stagnation zone for airflow, causing increased surface temperatures. Theoretically the radiation heat loss should be doubled as area is doubled. But as the inside cylinder provides kind of locking arrangement for reflected radiation which get blocked inside cavity and finally get absorbed. The added surface area is near to the bottom and hence has less view factor with aperture. As surface temperature are increase, conduction losses will be slightly increased. From energy balance, total losses from cavity must be equal to total power input as there is no working fluid, so convection losses will reduce.

Comparison of Radiation Heat Losses with Published Literature

The present study results for normal cavity and modified cavity with 150 W heat input using only side heaters was carried out with those of Abbasi-Shavazi et al. [2] as the setup and cavity dimensions along with cavity materials are same. The cavities considered was painted with pyromark 2500 solar grade. The Abbasi-Shavazi et al. [2] has used top wall temperatures for calculation of radiation heat losses and conduction heat losses. They also used radiosity method for calculation of radiation heat losses from cavity with axisymmetric assumptions. The present study uses average of minimum four temperatures recorded for each surface considered in radiosity network analysis and overall average surface temperate for side surface and bottom surface for conduction loss measurement. The comparison shows close agreement with similar trend for normal cavity with minimum deviation of 4.7% at 0° inclination and maximum deviation of 15.7 % at 90° inclination. The Abbasi results shows higher radiation heat losses as only top surface temperatures were used which are always higher compared to bottom side surface temperatures. The surface temperatures obtained by Abbasi are slightly higher may be due to use of different insulation, heating medium and environmental conditions which leads to higher radiation losses. The modified cavity shows similar trend as that of normal cavity with slightly higher losses due to higher surface temperatures. The comparison of radiation heat loss values with Abbasi-Shavazi et al. [2] results is shown in Figure 11.

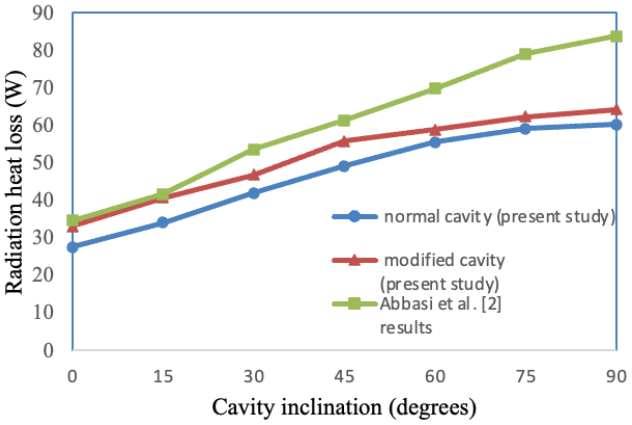

Figure 11. Comparison of radiation heat loss values with Abbasi-Shavazi et al. [2] results.

CONCLUSION

The radiosity network method was used to calculate radiation heat losses. The experimental setup was developed to measure the non-isothermal surface temperatures. For uniform surface temperature conditions, uniform radiosity consideration will always predict higher radiation losses compared to non-uniform radiosity over the cavity surface. The difference is more at lower temperatures and will remain uniform at 2.14 % for temperatures above 673 K. Though the surface area is doubled in the case of the proposed cavity, the radiation heat losses should be theoretically doubled, but due to lower view factors they slightly increased. The radiation heat losses remain nearly the same for all three temperature cases of the inner cylinder. Sensitivity analysis showed increased radiation heat losses with increasing emissivity. In case of increased aspect ratio, the increased surface area inside the cavity due to increased length will not contribute more due to its lower view factors.

Experimental results showing non-isothermal surface conditions, the proposed cavity shows slightly higher radiation heat losses than the normal cavity due to higher surface temperatures which is due to the increased stagnation zone for airflow inside the cavity caused by the inner cylinder. For 150 W input using side heaters, the radiation losses increased only by 4.5% for the proposed cavity at 15° inclination. As radiation losses and conduction losses increases slightly for modified cavity, by energy balance the convection losses will reduce to keep total heat loss equal to heat input. This means modified cavity will maintain higher working temperatures with same total heat loss as that of normal cavity. Increased temperatures represent higher heat availability for absorption which increase the thermal performance of receiver. So, the designer may think of a proposed cylinder-in-cylinder arrangement for improved thermal performance for cylindrical cavities along with ease of manufacturing and maintenance.

NOMENCLATURE

A	area
amb	ambient
A_{ap}	aperture area
A_w	internal cavity surface area
cond	conduction heat loss
D	diameter
D_{ap}	aperture diameter
D_{cav}	cavity diameter
E_b	emissive power of a black body
F_{ij}	view factor for surface i with surface j
h	height of interior convex
H	depth of cavity receiver
i	surface or section
J_i	radiosity of surface i
L	length of Cavity
L_3	length of inner cylinder of cavity
q_i	specific heat input flux for surface i
q_{ij}	radiation heat exchange between surface i and j
rad	radiation
R_i	radiative surface resistance for surface i
R_{ij}	radiative space resistance between surface i and j
T	temperature
T_{amb}	ambient temperature
T_w	average cavity wall temperature
w	wall

Greek symbols

ε	emissivity
σ	Stefan Boltzman Constant

ACKNOWLEDGMENT

The authors are very thankful to VJTI for providing the setup facility and financial support for this research. We are also thankful to M/s Padmatech Industries Pvt Limited, Pune and M/s Teja's Enterprises, Pune, M/s Pratik heat products, Mumbai, and M/s Geeta surface coatings Pvt Ltd, Pune, for providing support in the fabrication of set up, application and curing of Pyromark 2500 coatings.

AUTHORSHIP CONTRIBUTIONS

Authors equally contributed to this work.

DATA AVAILABILITY STATEMENT

The authors confirm that the data that supports the findings of this study are available within the article. Raw data that support the finding of this study are available from the corresponding author, upon reasonable request.

CONFLICT OF INTEREST

The author declared no potential conflicts of interest with respect to the research, authorship, and/or publication of this article.

ETHICS

There are no ethical issues with the publication of this manuscript.

REFERENCES

[1] Ameri M, Farhangian Marandi O, Adelshahian B. The effect of aperture size on the cavity performance of solar thermoelectric generator. J Renew Energy Environ 2017;4:39-46.

[2] Abbasi-Shavazi E, Hughes GO, Pye JD. Investigation of heat loss from solar cavity receiver. Energy Proc 2015;69:269-278. [CrossRef]

[3] Paitoonsurikarn S, Lovegrove K. Numerical investigation of natural convection loss in cavity-type solar receivers. Solar - Proceedings of 40th Australian and New Zealand Solar Energy Society ANZSES Conference, 2002, Australia. pp.1-6.

[4] Paitoonsurikarn S, Lovegrove K. On the study of convection loss from open cavity receivers in solar paraboloidal dish applications. Renewables - Proceedings of 41st Australia and New Zealand Solar Energy Society ANZSES Conference, 26-29 Nov 2003, Melbourne, Australia. pp.154-161.

[5] Alvarado-Juárez R, Montiel-González M, Villafán-Vidales HI, Estrada CA, Flores-Navarrete J. Experimental and numerical study of conjugate heat transfer in an open square-cavity solar receiver. Int J Therm Sci 2020;156:106458. [CrossRef]

[6] Maurya A, Kumar A, Sharma D. A comprehensive review on performance assessment of solar cavity receiver with parabolic dish collector. Energ Source Part A 2022;44:4808-4845. [CrossRef]

[7] Wu SY, Guan JY, Xiao L, Shen ZG, Xu LH. Experimental investigation on the heat loss of a fully open cylindrical cavity with different boundary conditions. Exp Therm Fluid Sci 2013;45:92-101. [CrossRef]

[8] Loni R, Asli-Areh EA, Ghobadian B, Kasaeian AB, Gorjian S, Najafi G, et al. Research and review study of solar dish concentrators with different nanofluids and different shapes of cavity receiver: Experimental tests. Renew Energy 2020;145:783-804. [CrossRef]

[9] Eterafi S, Gorjian S, Amidpour M. Effect of covering aperture of conical cavity receiver on thermal performance of parabolic dish collector: experimental and numerical investigations. J Renew Energy Environ 2021;8:29-41.

[10] Gonzalez MM, Hinojosa JP, Estrada CA. Numerical study of heat transfer by natural convection and surface thermal radiation in an open cavity receiver. Sol Energy 2012;86:1118-1128. [CrossRef]

[11] Juarezb JO, Hinojosa JF, Xaman JP, Tello MP. Numerical study of natural convection in an open cavity considering temperature-dependent fluid properties. Int J Therm Sci 2011;50;2184-2197. [CrossRef]

[12] Venkatachalam T, Cheralathan M. Effect of aspect ratio on the thermal performance of cavity receiver for solar parabolic dish concentrator: An experimental study. Renew Energy, 2019;139:573-581. [CrossRef]

[13] Yuan Y, Xiaojie L, Ziming C, Fuqiang W, Yong S, Heping T. Experimental investigation of thermal performance enhancement of cavity receiver with bottom surface interior convex. Appl Therm Engineer 2020;168:114847. [CrossRef]

[14] Bellos E, Bousi E, Tzivanidis C, Pavlovic S. Optical and thermal analysis of different cavity receiver designs for solar dish concentrators. Energy Conver Manage 2019;100013:1-19. [CrossRef]

[15] Reddy KS, Kumar NS. Convection and surface radiation heat losses from modified cavity receiver of solar parabolic dish collector with two-stage concentration. Heat Mass Transf 2009;45:363-373. [CrossRef]

[16] Reddy KS, Kumar NS. Combined laminar natural convection and surface radiation heat transfer in a modified cavity receiver of the solar parabolic dish. Int J Therm Sci 2008;47:1647-1657. [CrossRef]

[17] Ibrahim UK, Salleh RM. Application of network representation model for radiation analysis. Int J Chem Engineer Appl 2012;3:195-200. [CrossRef]

[18] Holman JP. Heat Transfer. 8th ed. New York: McGraw-Hill; 1997.

[19] Taumoefolau T, Paitoonsurikarn S, Hughes G, Lovegrove K. Experimental investigation of natural convection heat loss from a model solar concentrator cavity receiver. J Sol Energy Engineer 2004;126:801-807. [CrossRef]

[20] Maag G, Falter C, Steinfeld A. The temperature of a quartz/sapphire window in a solar cavity receiver. J Sol Energy Engineer 2011;133:014501. [CrossRef]

[21] Neber M, Lee H. Design of a high-temperature cavity receiver for residential-scale concentrated solar power. Energy 2012;47:481-487. [CrossRef]

[22] Zou C, Zhang Y, Falcoz Q, Neveu P, Zhang C, Shu W, et al. Design and optimization of a high-temperature cavity receiver for a solar energy cascade utilization system. Renew Energy 2017;103:478-489. [CrossRef]

[23] Bader R, Barbato M, Pedretti A, Steinfeld A. An air-based corrugated cavity-receiver for solar parabolic trough concentrators. Appl Energy 2010;138:337-345. [CrossRef]

[24] Hathaway BJ, Lipiński W, Davidson JH. Heat transfer in a solar cavity receiver: Design considerations. Numer Heat Tr A-Appl 2012;62:445-461. [CrossRef]

[25] Pye J, Hughes G, Abbasi E, Asselineau CA, Burgess G, Coventry J, et al. Development of a higher-efficiency tubular cavity receiver for direct steam generation on a dish concentrator. AIP Conf Proc 2016;1734:030029. [CrossRef]

[26] Gil R, Monné C, Bernal N, Muñoz M, Moreno F. Thermal model of a dish Stirling cavity-receiver. Energies 2015;8:1042-1057. [CrossRef]

[27] Abbasi-Shavazi E, Torres JF, Hughes G, Pye J. Experimental correlation of natural convection losses from a scale-model solar cavity receiver with non-isothermal surface temperature distribution. Sol Energy 2020;198:355-375. [CrossRef]

[28] Wang Y, Lipiński W, Pye J. A method for in situ measurement of directional and spatial radiosity distributions from complex-shaped solar thermal receivers. Sol Energy 2020;201:732-745. [CrossRef]

[29] Sinha R, Gulhane NP. Numerical study of radiation heat loss from solar cavity receiver of parabolic dish collector. Numer Heat Tr A-Appl 2020;77:743-759. [CrossRef]

[30] Wasankar KS, Yadav SC, Sinha R, Gulhane NP. Numerical investigation of heat losses through cascaded fully open cavity receiver at high temperatures (up to 500°C). E3S Web Conf 2019;128:01018. [CrossRef]